PHYSICS

Seed Money Fund

A Novel Device for Quantitative Single-Atom Detection of Carbon-14

F. W. Meyer
Physics Division

In this seed money project, the feasibility of developing a novel, compact apparatus for the quantitative detection of ^{14}C at the part-in 10^{12} level has been investigated. Carbon-14–labeled compounds are widely used in the pharmaceutical industry (e.g., as tracers to determine the fate of these compounds in vivo). Tracer studies of metabolic products in breath exhalations are used in the diagnosis of certain metabolic disorders. The sensitivities of most present methods are inadequate to permit utilization of sufficiently small quantities of ^{14}C to avoid the issues of radioactive waste and contamination, both of which are unacceptable for environmental, health and safety, and financial reasons. For these reasons, there is significant current interest in exploring other high-sensitivity ^{14}C detection methodologies that permit reduction of ^{14}C labeling to levels slightly above background. Conventional accelerator mass spectrometry (AMS) is at present the only approach that offers sufficiently high sensitivity to avoid the above-radiological issues, but it requires large-scale facilities that are usually not dedicated to a single task, with correspondingly high cost. The AMS technique further entails time-consuming sample preparation prior to the actual measurements and so is not suited to quasi–real time monitoring of ^{14}C levels.

Introduction

The natural abundance of ^{14}C in "modern" samples is about 1.18×10^{-12} per ^{12}C atom, and this determines the background level from which the levels of tracers used (e.g., in the pharmaceutical industry) must be distinguishable. The main difficulty in single-atom detection of ^{14}C arises from the isobaric interferences due to atomic ions (e.g., ^{14}N) and molecular ions (e.g., $^{12}CH_2$ and ^{13}CH). In conventional AMS,[1] the approach consists of using a negative ion source to eliminate the ^{14}N contamination, since it does not support a stable negative ion, accelerating the negative ion beam in a tandem accelerator to high energy (few MeV), and then dissociating molecular ions isobaric with $^{14}C^-$, also present in the ion beam, either in a foil or gas target. Subsequent stages of electrostatic and magnetic analysis are then used to isolate the ^{14}C ions before their detection. Conventional AMS requires large facilities, usually not dedicated to a single task, with correspondingly high cost, and entails time-consuming sample preparation prior to the actual measurements.

Technical Approach

For the present proof-of-principle project, the ORNL Multicharged Ion Research Facility (MIRF)[2] electron cyclotron resonance (ECR) ion source was used for the production of a multicharged carbon beam with charge state of +3 or higher to eliminate molecular isobar interference at mass 14. After magnetic selection of the desired charge state, the multicharged ion beam, which will still be dominated by ^{14}N multicharged ions of the same charge state, is directed at grazing incidence on a LiF single-crystal surface, where efficient negative ion formation takes place without appreciable energy loss of the scattered beams. The different scattered charge states are dispersed in the first stage of a large-acceptance-angle, two-stage electrostatic analysis system. The second, high-resolution, stage further spatially separated the desired $^{14}C^-$ ions from other scattered charge states prior to their detection on a two-dimensional, position-sensitive detector (2-D PSD). The analysis system transmitted more than 50% of the negatively charged projectiles produced during the grazing scattering interactions with the LiF surface. Since ^{14}N does not form a stable negative ion, interference due to ^{14}N could be effectively eliminated. Unique characteristics of the apparatus are its small size, low cost, high efficiency (i.e., throughput), and ease of sample preparation, in comparison to conventional AMS hardware. As a result, this apparatus[3] should find great utility in such applications as quasi–real time monitoring of ^{14}C-based chemical tracer uptake in biological systems, atmospheric pollution studies, cancer research, medical diagnostics, and other biomedical studies.

Results and Accomplishments

During FY 2001, a careful analysis of the mass rejection capability of the ORNL MIRF magnetic analysis system was performed. It was verified that adjacent mass

rejection is more than sufficient to meet the stringent requirements of this project. In addition, the 2D-PSD used in the final stage of ^{14}C detection (i.e., after the negative ion formation by surface scattering) was extensively refurbished and prepared for installation into the surface scattering chamber.

During FY 2002 the detailed design and fabrication of the ^{14}C detection apparatus, shown schematically in Fig. 1, were carried out. The work performed included design and fabrication of a large-area LiF sample mount that was heatable to 400°C. The sample holder, shown in Fig. 2, is supported by a 3-axis goniometer with rotation to permit accurate orientation relative to the incident multicharged ion beam. In addition, two large-acceptance, spherical-sector electrostatic deflectors were designed and fabricated. The first, a 45° analyzer, served to separate the negatively charged ^{14}C ions produced by the grazing interaction with the LiF target from the dominant scattered neutral ^{14}N flux. The second, a higher resolution 90° analyzer, served to energy-analyze the desired negatively charged ^{14}C ions prior to detection for further signal-to-noise enhancement. Both analyzers are double-focusing and thus permit maximum collection rate of the desired ions. To house these analyzers and detector, suitable vacuum chambers were designed and fabricated as well.

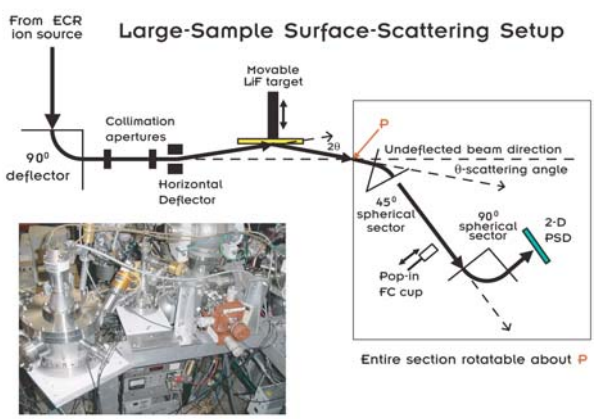

Fig. 1. Schematic of the ^{14}C detection apparatus developed for this project. The scheme entails grazingly scattering up to 3-mm-diam, μA-intensity ion beams from a large single-crystal sample, and a two-stage, large-acceptance-angle, double-focusing analysis for separation of $^{14}C^-$ ions produced during the grazing surface interactions from the more intense scattering products.

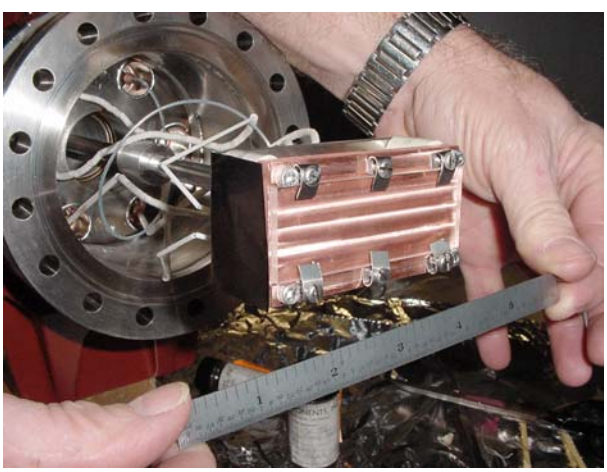

Fig. 2. Large sample mount showing 69-mm × 29-mm × 3-mm cleaved LiF target mounted on a heated sample stage capable of being heated to 400°C.

During FY 2003 the apparatus was assembled and tested. Beam currents of 0.2–0.5 pμA of $^{12}C^{q+}$ (q = 2–4) were achieved on the large LiF sample at incidence angles as low as a few degrees. The grazing scattering interactions produced up to 20 pnA of $^{12}C^-$. The observed C^- yield was found to be significantly lower than expected on the basis of our earlier O^- production measurements[3] but still corresponded to a particle flux of about 1.2×10^{12}/s. From the natural abundance of ^{14}C quoted earlier, this translates to a $^{14}C^-$ flux of about 0.2 Hz. However, background events were found to dominate the $^{14}C^-$ count rate by about two orders of magnitude. The smaller-than-expected C^- yield was found to be due to a subtle atomic physics effect having to do with differences in the statistical weights of the neutral parent states from which C^- and O^- can be formed.[4] Choice of an alkali halide target with a higher-lying valence band is expected to increase the yield at least a factor of two. The source of the above noted background was found to be F^- sputtered particles. Due to the close mass proximity of mass-14 projectiles and the mass-19 F target constituents, the maximum energy of the sputtered F^- particles E_{sp} is very close to the primary beam energy E_0 ($E_{sp} = 0.977\ E_0$). As a result the F^- particles could not be effectively discriminated against in the second electrostatic analyzer and thus resulted in the observed background,[5] as shown in Fig. 3. By using a heavier alkali halide target, such as RbI, both the low-negative-ion yield and sputtered-particle background problems can be eliminated. The top of the valence band of RbI lies almost 6 eV higher in energy than LiF. Also, with its much higher halogen mass (iodine is mass 127), the maximum energy of sputtered I^- particles will be only about one-third of the primary beam energy, which can thus be effectively discriminated against in the second analyzer. As illustrated in Fig. 4, already for mass-40 incident projectiles, for which the maximum sputtered F energy is reduced to about 88% of the primary beam energy, the mass-14 backgrounds were found to be reduced by more than two orders of magnitude to levels less than 1 Hz.

Summary and Conclusions

In this project, proof-of-principle of a low-energy, compact scheme for quantitative ^{14}C detection has been successfully demonstrated. The next stage of development

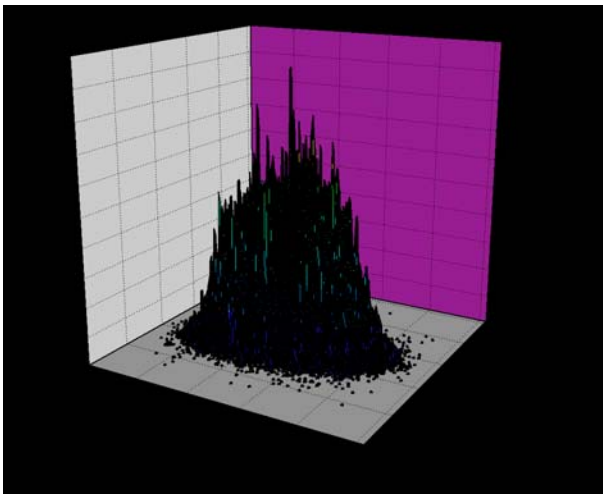

Fig. 3. Intensity distribution on the 2-D PSD when 27-keV triply charged mass-14 ions of μA intensity are incident on the LiF target; the high background is due to full-energy F^- sputtered particles indistinguishable from $^{14}C^-$ ions of the same energy produced during the grazing LiF surface scattering.

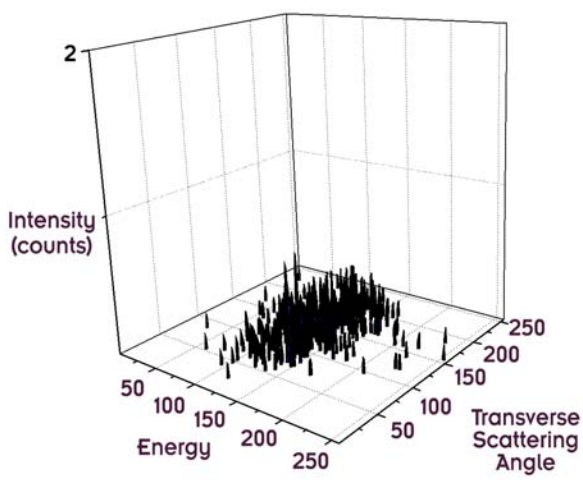

Fig. 4. Intensity distribution on the 2-D PSD when 27-keV mass-40 ions are incident on the LiF target; note greatly reduced background due to absence of full energy F^- sputtered particles.

can therefore now be envisioned. Together with implementation of a heavier alkali halide target such as RbI to increase the negative-ion yield and to greatly reduce background levels, the use of a compact all-permanent magnet ECR source could result in a truly table-top-size system. The addition of front-end delivery systems to handle real-time introduction of liquids and combustion products into the ECR source would make this device of great utility in the pharmaceutical industry or as a biomedical research tool. Accelerator mass spectrometry (AMS) is the only presently available method sufficiently sensitive to permit utilization of sufficiently small quantities of ^{14}C to avoid the issues of radioactive waste and contamination, both of which are unacceptable for environmental, health, and safety and financial reasons. AMS facilities, however, are expensive, not portable, and do not have real-time processing capability. For these reasons, the pharmaceutical industry is currently exploring other high-sensitivity ^{14}C detection methodologies that permit reduction of ^{14}C labeling to levels slightly above background.

A proposal for further development of the approach demonstrated in this project will be prepared for submission to the DOE Office of Biological and Environmental Sciences or NIH. Subsequently or alternatively, an industrial partner could be sought for commercialization. The apparatus developed in this manner should find broad application in biomedical research using ^{14}C tracers, and, with some sensitivity enhancement, in tracer studies of atmospheric chemistry and transport, ocean mixing, erosional processes and glacial recession, diffusion through soils, diesel exhaust pollution, lubricant consumption and degradation, wear analyses of graphite composite materials, and various petroleum industry problems.[6] One local application of the device could be in the ecosystem-scale ^{14}C pulse labeling experiment on carbon sequestration in soil,[7] made possible by the 1999 ^{14}C release from one of the Oak Ridge Reservation incinerators. If sufficient improvement in sensitivity over the initial design goal (10^{-12}) is achieved, then additional possibilities might include radiocarbon dating applications in the areas of paleoclimatology and archaeology.

References

[1]D. Elmore and F. M. Philips, *Science* **236**, 543 (1987).

[2]F. W. Meyer, "ECR-based Atomic Collision Physics Research at ORNL MIRF," in *Trapping Highly Charged Ions: Fundamentals and Applications,* J. Gillaspy, ed., Nova Science Pub, New York, 2000, pp. 117–164.

[3]U.S. patent 6,455,844, issued September 24, 2002.

[4]F. W. Meyer, Q. Yan, P. Zeijlmans van Emmichoven, I. G. Hughes, and G. Spierings, *NIM* **B125**, 138 (1997).

[5]F. W. Meyer, "A Novel Device for Quantitative Single-Atom Detection of Carbon-14," Book of Abstracts, XXIII ICPEAC, Stockholm, Sweden, July 23–29, 2003.

[6]J. C. Davis, *NIM* **B*92*,** 1 (1994).

[7]"Carbon-14 levels discovered on ORR provide a unique scientific opportunity," *ORNL Reporter*, Issue 44, p. 1, December 2002.

A Miniature Electrostatic Molecular-Ion Storage Ring

M. E. Bannister and D. R. Schultz
Physics Division

Cold molecular ions are needed to experimentally determine key collision rates required for fundamental physical and chemical studies, fusion energy research, aeronomy, astrophysics, lighting, and plasma processing, for example. The objective of this project has been to produce proof of concept for a novel, compact source of molecular ions which can very cost-effectively produce rotationally/vibrationally cold molecular ions necessary for research underpinning these diverse applications. In brief, molecular ions were formed in a surface-wave plasma source where their internal temperature is lowered through adiabatic cooling in a supersonic expansion. The feasibility of injecting these ions into a small, cryogenically cooled electrostatic storage ring was studied. Storage for milliseconds in the cooled ring would allow radiative relaxation of the ions' excited states, further cooling them to the temperatures required for fundamental and applied investigations. Alternative technologies rely on large magnetic or electrostatic storage ring facilities that cost hundreds of thousands to millions of dollars and are not presently available in the United States.

Introduction

European nations and Japan invested significant funds in heavy-ion storage rings with electron cooling in the last two decades while the United States did not, forcing U.S. researchers seeking to perform atomic and molecular physics experiments enabled by these devices to request and compete for time abroad. In addition to experiments exploring electron-atomic-ion collisions, the rings have made possible study of collisions of electrons with cool molecular ions. Cooling of the internal vibrational energy of the molecular ion proceeds by injecting ions from an ion source and allowing them to circulate in the ring long enough to radiate away their internal energy. Studying such collisions is central to understanding processes in a wide range of environments including fusion reactors, astrophysical and aeronomical plasmas, lighting, and technical plasma processing devices.

In particular, we focused on demonstration of proof of concept for a cool molecular ion source coupled to a miniature electrostatic storage ring that is extremely compact and inexpensive compared to existing rings. This device could bring a significant capability to ORNL and to the U.S. research community, opening opportunities for key research now only possible using large, foreign storage-ring facilities. The development steps included the design and testing of a novel cool ion source, simulation of the storage ring operation, assembly of the small electrostatic ring, and testing of the output performance (e.g., ion temperature, beam intensity, collimation) of the device via spectroscopic measurements.

Technical Approach

A key component of this project is the source that produces the cool molecular ions to be stored in the miniature electrostatic storage ring. The molecular ions are formed in a surface-wave-sustained discharge that is expanded adiabatically into vacuum through a supersonic nozzle. Microwaves propagated from a waveguide launching structure called a surfatron supply the energy necessary to maintain the plasma column. These surface waves travel down the discharge tube, which is effectively a plasma waveguide, and, if sufficient microwave power is applied, reach the supersonic nozzle at the end of the tube. For given flow conditions in the expansion, determined by the nozzle diameter and the gas pressure in the tube, the plasma parameters such as electron density and temperature can be controlled in the nozzle and expansion region by adjusting the microwave power. The microwave circuit of the surfatron launcher has three separate adjustments to optimize the coupling of the microwaves to the plasma column so that the reflected power from the surfatron is typically less than 5% under operating conditions.

The supersonic nozzle was formed at the end of the 4.0-mm-I.D. quartz tube by heating the end of an open tube until it drew closed on itself. This closed end was then ground away until a small opening, less than 100 μm in diameter, was made. During source operation, the nozzle end of the discharge tube was cooled by distilled water sent through a coaxial cooling jacket by a refrigerated circulator. Additional cooling of the surfatron and discharge tube were provided by a combination of chilled water and forced air.

Extraction of the molecular ions from the supersonic expansion region was accomplished by an small metal annulus located around the nozzle end of the discharge tube. Application of a voltage of up to a few kilovolts on this annulus forced the ions away from the nozzle where they were focused into a beam by a cylindrical lens. Using additional cylindrical lenses and deflectors, the beam was transported more than 1 m to either a Faraday cup used for total current measurements or to a channel electron multiplier used for time-of-flight (TOF) beam diagnostics. Short bunches of ions used in the TOF measurements were produced by rapidly pulsing (pulse width ~300 ns) the voltage on one of the ion deflectors to allow ions to pass only during a narrow window of time.

Results and Accomplishments

We summarize here some typical results from the characterization of the surfajet ion source. The dependence of the plasma parameters in the nozzle expansion region on the absorbed microwave power was evidenced by measurements of the total ion current as a function of power. Figure 1 shows this dependence for a nitrogen discharge with a pressure of 1.2 Torr expanding through an 84-µm-diam nozzle. Until the absorbed power reaches approximately 810 W, essentially no ions survive into the expansion. As the power increases above that threshold level, the ion current extracted at 1 kV increases linearly. Emission of visible light from the discharge extends all the way to the nozzle for power levels above this critical value. These two observations strongly suggest that in order for ions to exist in the expansion region, sufficient microwave energy must propagate past the nozzle end of the discharge to continue ionizing the gas, because ions formed before the nozzle recombine due to collisions in the nozzle.

Time-of-flight spectra were recorded for various levels of power above the threshold for the discharge conditions described above. Two such spectra are shown in Fig. 2 with power levels corresponding to points labeled A and B on Fig. 1. For an absorbed power just above the threshold value for ion production, the TOF spectrum (dashed curve in Fig. 2) shows only molecular ions, namely N_2^+ and impurity H_2O^+. At the higher power level, the TOF spectrum (solid curve in Fig. 2) also shows the presence of atomic ions, N^+, comprising approximately 12% of the extracted beam. Despite the obvious change in plasma parameters in the expansion region, no difference was seen in the width of the molecular ion peak, which is related to the translational temperature of the beam.

The miniature electrostatic molecular-ion storage ring was simulated in three dimensions using the computer program SIMION.[1] The base design was a scaled-down version of an electrostatic ion storage ring operating in Japan.[2] Results from these simulations indicated that building such a miniature ring with a circumference of 1.4 m was feasible provided that electrodes were machined and assembled with sufficient accuracy. It was determined that the addition of cryogenic cooling to the elements of the ring, however, would greatly increase the complexity of the construction and operation.

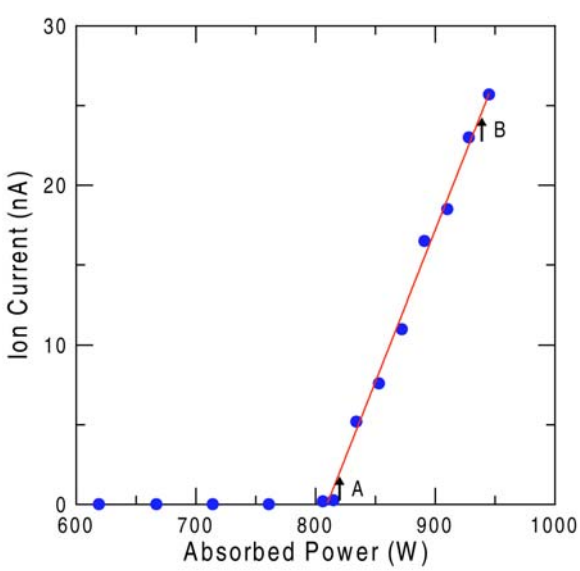

Fig. 1. Total current extracted at 1 kV from the surfajet molecular ion source as a function of the microwave power absorbed in a surface-wave-sustained nitrogen plasma. The gas pressure was 1.2 Torr and the supersonic nozzle had a diameter of 84 µm.

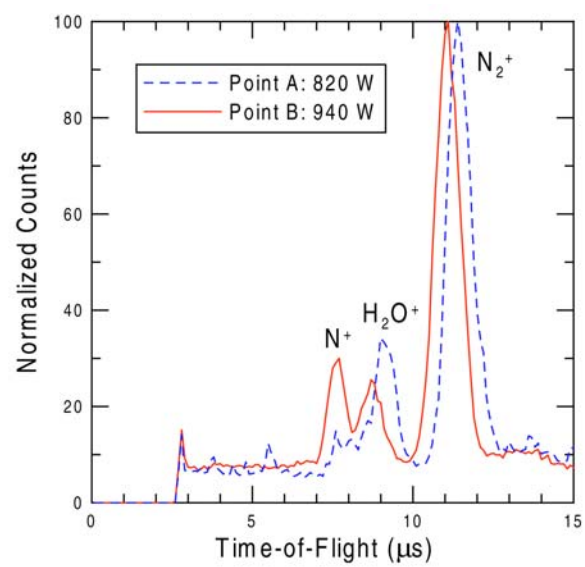

Fig. 2. Time-of-flight spectra for ion beams extracted at 1 kV from the surfajet molecular ion source. The dashed curve was measured for 820 W absorbed power (labeled point A on Fig. 1); the solid curve was for 940 W absorbed power (point B on Fig. 1).

Summary and Conclusions

The development of the surfajet source for cool molecular ions yielded beams sufficient for injection into a miniature electrostatic ion storage ring or for separate collision experiments (greater than 100 nA at 1-keV energy). Time-of-flight diagnostics on the extracted beams were inconclusive about the degree of cooling of the ions by the supersonic expansion; follow-on spectroscopic measurements will be required to quantify the internal cooling of the extracted ions. Simulations of the miniature electrostatic ion storage ring showed the feasibility of such a device, but the time and funding required turned out to be beyond the scope afforded by this project.

Once the internal cooling of the molecular ions is fully characterized, the surfajet source is quite suitable for collision experiments with electrons, atoms, and surfaces. It can be adapted for use on the high-voltage ion source platform under construction at the Multicharged Ion Research Facility in the ORNL Physics Division, making a variety of cool, well-characterized molecular ions available at energies up to 250 keV for experiments such as measurements of dissociative recombination, excitation, and ionization by electron impact.

This project on development of a cold molecular-ion source has already led to additional funding from the DOE Office of Basic Energy Sciences (OBES) at a level of $200K/year for the study of electron-impact dissociation of molecular ions. This OBES-funded experimental program includes support for continued research on characterization and optimization of the surfajet as a source of cold molecular ions. A well-characterized source will also be advantageous for pursuit of future funding from NASA for experiments on cold molecular ion species of astrophysical significance.

References

[1]D. A. Dahl, *SIMION 3D Version 7.0*, INEEL-95/0403, Idaho National Engineering and Environmental Laboratory, Idaho Falls, Idaho, 2000.

[2]T. Tanabe, K. Chida, K. Noda, and I. Watanabe, "An Electrostatic Storage Ring for Molecular Science," pp.797–799 in *Proceedings of the Seventh European Particle Accelerator Conference*, ed. M. Regler, 2000.

Ultrafast-Laser-Produced Radioactive Ions

C. R. Vane,[1] Y. Liu,[1] H. F. Krause,[1] J. R. Beene,[1] D. R. Schultz,[1] K. Flippo,[2]
A. Maksimchuk,[2] and D. Umstadter[2]
[1]*Physics Division, ORNL*
[2]*Center for Ultrafast Optical Science, University of Michigan, Ann Arbor, Michigan*

Significant production of radioactive isotopes that can be used in fundamental research or for medical purposes has been demonstrated through novel experiments in which the isotopes were created by nuclear reactions driven by light particles accelerated in ultrafast/ultra-intense laser irradiation of solid targets. Measurements were carried out to explore optimization of yields of several radioactive species by choice of laser parameters, as well as driver target materials and geometries. These experiments were accomplished and yield results were made absolute using detailed diagnostics and analyses based on nuclear spectroscopy of the produced radionuclides.

Introduction

Short-lived radioisotopes and ions (that is, ions with unstable nuclei) are of intrinsic interest in nuclear physics, of great importance in astrophysics, and of great practical use, particularly in medical applications. Consequently, research centers such as ORNL's Holifield Radioactive Ion Beam Facility (HRIBF) are dedicated to producing these exotic species and exploring in detail their properties. In addition, hospitals and medical research facilities generate short-lived radiotherapeutic and diagnostic isotopes by using commercial cyclotrons or by collecting radioactive samples generated at nuclear reactors. The focus of the work initiated here was aimed at exploring and potentially creating a new source for radioisotopes and ion beams (RIBs) based on laser acceleration of light particles. Such sources may have many significant advantages over conventional methods for producing these isotopes.

The recent advent of ultrafast (femtosecond pulses), ultra-intense (multiterawatt or higher) lasers has unexpectedly lead to the observation of highly accelerated, well-collimated electron and proton beams emanating from solid, gas, and cluster targets subjected to high-power laser pulses. The ultra-intense laser pulses rapidly accelerate electrons within the target, creating charge separation and enormous transient electric and magnetic fields. The electric fields accelerate protons or deuterons occupying hydrogen-bearing surface layers on the target. These discoveries have opened the possibility of creating compact, efficient sources of radioisotopes using the laser-accelerated lighter particles as drivers of nuclear reactions in isotope production targets.[1] The very rapid advances being made in capabilities of ultrafast/ultra-intense lasers also greatly leverage development and future performance of any ultrafast-laser-produced radioisotope source.

Technical Approach

Our approach was to develop the technology necessary for proof-of-concept production of several short-lived radionuclides through the use of intense (10-TW), ultrafast (400-fs) pulses of laser light focused on solid targets. Protons and deuterons accelerated to high energies by interaction of the laser pulses focused on these primary driver targets were used to bombard secondary targets and produce radioactive isotopes.

Simulation studies were performed at ORNL for optimized production of several potential radioisotopes from laser-driven high-energy proton and deuteron impact on elemental targets, as well as for extraction of the fraction of radioactive ions transmitted during recoil out of thin targets. Calculations were also performed to give expected yields of the radioactive ions that could be slowed in a He buffer gas and then extracted using electric fields. Expertise at the HRIBF was used to establish reliable calculations of ion beam extraction from high-energy impact on isotope targets, using methods employed for cyclotron-accelerated protons. Following these simulations, an apparatus was designed and constructed and three experiments were carried out at the Center for Ultrafast Optical Science (CUOS), University of Michigan at Ann Arbor. These experiments were performed in collaboration with Professor Donald Umstadter and his colleagues at the University of Michigan, especially Kirk Flippo, whose Ph.D. thesis (2003) was based partly on work in this project. The measurements were all performed using 1.053-nm, 10-TW, 400-fs laser pulses from a hybrid

Ti:sapphire/Nd:phosphate glass chirped pulse amplification laser to accelerate protons and deuterons out of thin-foil driver targets and onto isotope production targets. The laser was focused before each shot (~7 min between shots) to approximately 6-µm spot diameter. The corresponding maximum focused intensity was ~4×10^{18} W/cm^2.

All exposures were performed in vacuum. The isotope production targets were either counted in place or extracted from the vacuum chamber and monitored for nuclear-decay gamma-ray emission using scintillation detectors. Measured yields of specific gamma rays were then used to calculate production yields of the identified isotopes. Employing appropriate nuclear cross sections, estimates were also extracted for the initial fluences of the respective accelerated particles (*p* or *d*) driving the nuclear reactions. With these in hand, one can estimate production yields for a much wider range of interesting radionuclides.

Protons and deuterons were accelerated to MeV energies by laser pulses focused on the front surfaces of thin mylar, aluminum, copper, and titanium foils. The basic setup is shown in Figs. 1 and 2. The deuteron surface coatings were produced either by laying down a layer of deuterated polystyrene in solution on mylar or aluminum foils, or by covering aluminum foils with a thin layer of sublimated titanium and then backfilling with deuterium gas to produce a few monolayers of TiD. Foil thicknesses typically ranged from 1 to 50 µm. The laser-ejected protons and deuterons from these thin foils were directed onto thick isotope production targets of enriched ^{11}B, or naturally occurring ^{12}C or ^{63}Cu to produce radioisotopes ^{11}C, ^{13}N, or

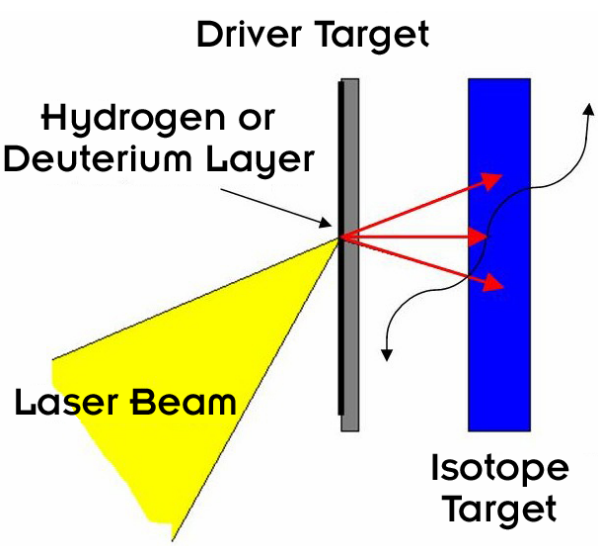

Fig. 1. Schematic of the two-step process for radionuclide production using ultrafast, ultra-intense lasers. The laser is focused on a thin driver foil where protons or deuterons are accelerated to high energy and emitted from the opposite side normal to the primary target. The fast particles are directed to a second isotope production target chosen to yield the selected radioisotope.

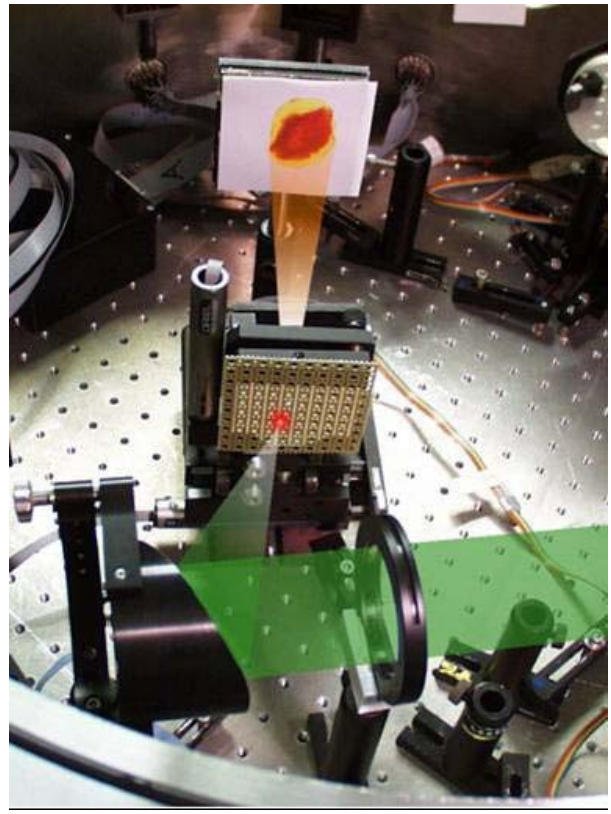

Fig. 2. Collimated beams of fast protons, observed from light emitted by passage through the vacuum chamber rest gas. The protons, which originate either from hydrogen-bearing impurities or from implanted deuterium on the front side of the target, are accelerated and exit the back side in a direction normal to the target surface. Electric field gradients ~10 GV/cm are inferred from measured maximum proton energies (up to ~5 MeV), which can be explained by charge separation due to "vacuum heating."

^{63}Zn, respectively. Gammas rays emitted from the decaying radioisotopes after a laser shot were initially counted in-place inside the vacuum chamber by NaI scintillations detectors located there, but the exceptionally high electromagnetic noise echoing after the shots and activation of the NaI materials made this method untenable. A target transport apparatus was constructed to permit fast extraction and retrieval of the isotope targets, and gamma-ray counting was carried out using Ge(Li) or NaI detectors mounted in a relatively noise-free environment outside the chamber after each laser pulse.

To optimize target material thickness for production of fast protons, tests were performed using a Thomson combined electric and magnetic field spectrometer[2] constructed by Kirk Flippo at the University of Michigan to roughly measure the accelerated heavy-particle energy distributions. For the conditions of this laser system, the proton yield-optimized thickness was found to be approximately 12.5 µm for aluminum foils. These thicknesses were subsequently used in measurements of

radioisotope production from a variety of driver target materials (mylar, Al, Ti, and Cu), again to examine effects on radioisotope production through (p,n) and (d,n) reactions.

Several previous researchers examining pulsed laser heavy-ion acceleration have shown that protons on the driver-target surface inhibit production of high-energy particles of any other species.[3] To reduce the hydrogen-bearing material contamination on thin metal targets, some of the foils were heated prior to laser exposure. In an attempt to observe these effects, we performed $^{12}C(d,n)^{13}N$ reaction yield measurements using 12.5-µm-thick aluminum foils coated with a deuterium-loaded titanium layer as a function of driver-target temperature. The driver foils were tested at temperatures from 20 to 210°C using a resistive heater attached to a copper mounting frame. The thick carbon isotope target used was maintained at 20°C.

Results and Accomplishments

Results of these studies to optimize high-energy particle acceleration and subsequent radioisotope production will be reported in a number of forthcoming publications,[4–6] For all the isotopes examined here, decays proceed primarily by positron emission. Subsequent annihilation of the beta leads to emission of two 511-keV gammas from the targets. Coincident counting of the 511-keV gammas was performed for each target over several lifetimes of the respective radionuclide. Time-dependent yields of singles and coincident 511-keV gammas were corrected for counting efficiencies and converted to initial numbers of the decaying parent nuclei. For the (p,n) reaction-generated nuclei and targets at room temperature, the best measurements gave approximately 10^5 radioactive ^{11}C and ^{63}Zn atoms produced per laser shot via $^{11}B(p,n)^{11}C$ and $^{63}Cu(p,n)^{63}Zn$ reactions, respectively. Identifications of specific isotopes were confirmed by decay rates of the gamma-ray singles rates. Figures 3 and 4 show examples of measured time dependences of the gamma-ray count rates for these isotopes.

For the (d,n) reaction–generated ^{13}N nuclei, where the target material (aluminum) and thickness (12.7 µm) were optimized, approximately 4×10^5 radioactive ^{13}N were produced per laser shot via $^{12}C(d,n)^{13}N$. We concentrated somewhat on improving production of these isotopes because ^{13}N is of special interest for nuclear astrophysics studies of hot CNO fusion cycle stars. We note that in contradiction to prior expectations, no enhancement in ^{13}N production was observed for aluminum driver targets heated to 210°C, although this temperature may not have been high enough to effectively remove all hydrogen contamination in the poor vacuum conditions experienced in the target chamber(~10^{-5} Torr).

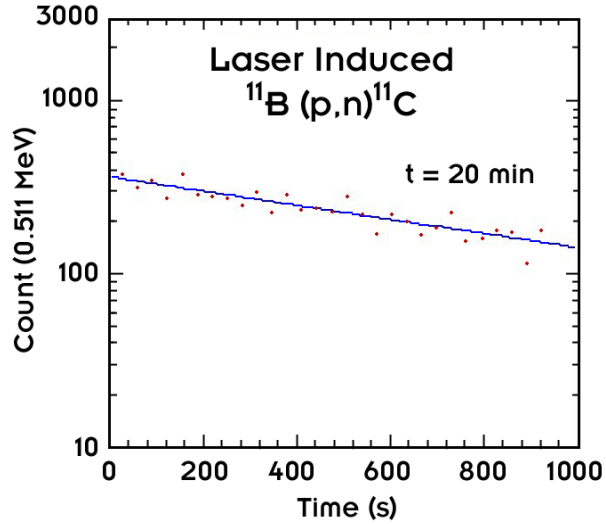

Fig. 3. Measured 511-keV gamma counts vs time after laser shot for decay of ^{11}C from $^{11}B(p,n)^{11}C$.

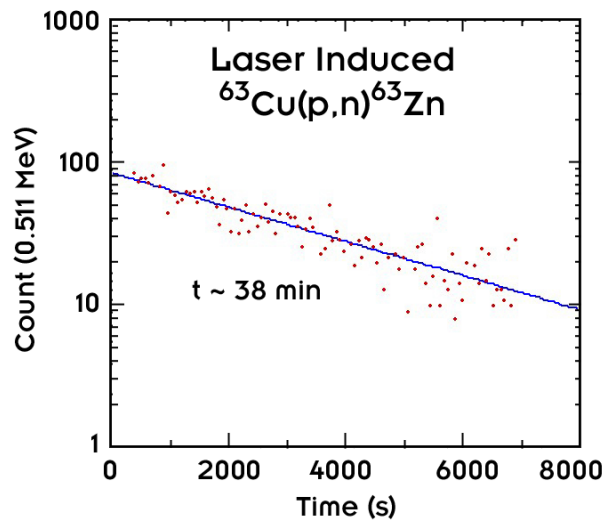

Fig. 4. Measured 511-keV gamma counts vs time after laser shot for decay of ^{63}Zn from $^{63}Cu(p,n)^{63}Zn$.

The ~10^5 ^{11}C, ^{13}N, and ^{63}Zn produced per laser shot represent a significant yield of radioactive nuclei, especially for multi-hertz laser systems. Assuming 10 pulses per second, as planned for a new laser system presently installed and undergoing initial testing at CUOS, the yield will conservatively be ~10^6/s, and result in equilibrium production of ~10^9 ^{13}N in a few tens of minutes. Similar yields of other important isotopes will also be possible.

From the measured isotope yields and known (p,n) and (d,n) cross sections, one can extract approximate incident intensities of the accelerated protons and deuterons. For example, $^{12}C(d,n)^{13}N$ is especially simple, since the cross section is essentially constant with deuteron

energy above about 0.8 MeV at 150 mb, as shown in Fig. 5. Assuming a deuteron energy distribution inferred from measurements for protons (actually, essentially half the proton end-point maximum energy), and correcting for energy loss in the isotope production ^{12}C target, we estimate that approximately 10^9 deuterons above 0.8 MeV were generated per laser pulse. That corresponds to a particle current of $\sim 10^{20-21}$/sec emitted from a ~10-µm spot during the few psec duration of particle emission after the laser pulse!

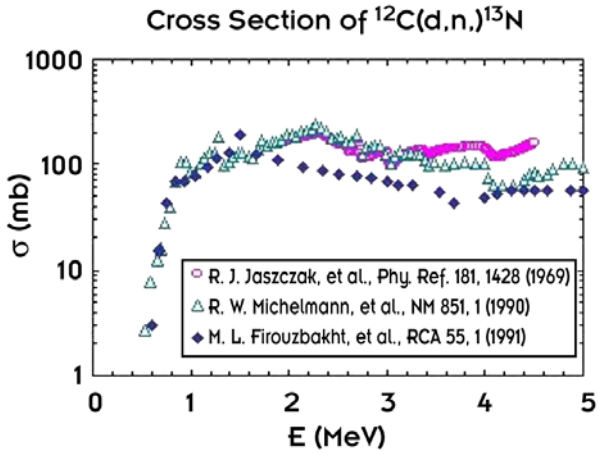

Fig. 5. Measured cross sections for deuteron impact $^{12}C(d,n)^{13}N$ reaction.

Summary and Conclusions

As demonstrated in this project, tabletop-sized, high-intensity, ultrafast pulse lasers have the potential for successful applications as sources of radioisotopes and, potentially, as high-quality ion beams of these isotopes. Higher laser power results in higher yields of accelerated particles and higher maximum energies, which will also make thicker isotope production targets and radionuclide yields possible. Similar experiments and simulations at larger, higher-power facilities have indicated that useful GBq quantities of short-lived medical isotopes (e.g., ^{11}C and ^{19}F, important for positron-emission tomography, for example) can be produced using 1-kHz lasers, perhaps available as tabletop systems only a generation or so away.[7]

The experience and results gained here have had significant influence on plans for future applications of laser-based radioactive ion beams. A new Field Work Proposal (ERKBL01 "Research and Development in Support of RIA") has been submitted to DOE Office of Nuclear Physics, based on research toward development of laser ion sources for radioactive ion beams (RIBs). Research outlined in this proposal concentrates on using laser resonance ionization properties for selectivity in extraction of RIBs produced by proton impact from high-energy accelerators. However, future work may also address laser pulse influence in direct production and preferential magnetic selection and acceleration of selected species.

More work is also planned to explore the feasibility of using high-quality, multi-MeV electrons generated by intense laser pulses on solid and gas targets for production of bremsstrahlung photons. Photonuclear reactions initiated by these high-energy photons have been studied rigorously for bremsstrahlung produced by electrons from accelerators. Photofission reactions of heavy nuclei are the only known mechanisms for producing neutron-rich isotopes, which are of primary interest to HRIBF researchers.

References

[1]K. Nemoto, A. Maksimchuk, S. Banerjee, K. Flippo, G. Mourou, D. Umstadter, and V. Y. Bychenkov, "Laser-triggered ion acceleration and table top isotope production," *Applied Physics Letters* **78**, 595 (2001).

[2]M. J. Rhee, "Compact Thomson Spectrometer," *Rev. Sci. Instrum.* **55**(8), 1229–1234 (1984).

[3]M. Hegelich et al., "MeV Ion Jets from Short-Pulse-Laser Interaction with Thin Foils," *Phys. Rev. Lett.* **89**, 085002 (2002).

[4]A. Maksimchuk, K. Flippo, H. Krause, G. Mourou, K. Nemoto, D. Shultz, D. Umstadter, R. Vane, V. Y. Bychenkov, G. I. Dudnikova, V. F. Kovalev, K. Mima, V. N. Novikov, Y. Sentoku, and S. V. Tolokonnikov, "High-Energy Ion Generation by Short Laser Pulses," *Plasma Phys. Rep*. (submitted).

[5]K. Flippo, T. Lin, V. Wong, M. Rever, K. Nash, A. Maksimchuk, and D. Umstadter, "Dependence of High-Intensity Laser Produced Proton Beams on Target Material Properties," *Phys. Rev. Lett.* (submitted).

[6]K. Flippo, A. Maksimchuk, T. Lin, M. Rever, and D. Umstadter, "Detailed Study of Deuteron and Heavier Ion Species Acceleration from Front and Rear Surfaces of High-Intensity Thin-Film Target Interactions," *Phys. Rev. Lett* (to be submitted).

[7]S. Fritzler, et al., "Proton Beams Generated with High-Intensity Lasers: Applications to Medical Isotope Production," *App. Phys. Lett.* **83**, 3039 (2003).

Density Matrix Renormalization Group for Interacting Fermions

T. Papenbrock, T. Barnes, D. J. Dean, and M. R. Strayer
Physics Division

Within this project we developed a numerical program (Fortran 90 code) based on the density matrix renormalization group (DMRG) to compute the low-lying states of spin chains and quantum dots with high accuracy. As an application, we investigated the critical behavior of the alternating spin-1/2 antiferromagnetic Heisenberg chain and computed the critical exponents of the ground-state energy defect and the excitation gap as the uniform chain is approached. We also applied the DMRG for electronic structure calculations in quantum dots and gave a proof-of-principle of this method.

Introduction

Fermions are the relevant degrees of freedom in physical systems ranging from macroscopic materials (metals and semiconductor devices) through mesoscopic and nanoscale electronic structures down to subatomic systems such as nuclei and hadrons. Understanding these dynamical multifermion systems is greatly complicated by the presence of interparticle interactions, which induce strong correlations in the many-body wave function of the system. As a result, simple approaches, such as mean field theory, fail to give an accurate description of many physical properties. In quantum dots, for example, it is now understood that fluctuations in conductance peak spacings cannot be understood in a mean field description. Another interesting example is given by quantum spin chains that exhibit critical behavior. At a critical point, the correlation length diverges and the theoretical description requires the understanding of many degrees of freedom.

Ab initio calculations of the properties of such systems are usually restricted to a rather small number of active fermions, since the exact diagonalization have computer memory and CPU time requirements that grow exponentially with system size. This exponential growth implies that the size of the system that can be treated using these traditional methods increases rather slowly with improvements in computer hardware. Although the use of Monte Carlo techniques allows the approximate solution of much larger Bose problems than can be treated using exact methods, when applied to dynamical fermion systems the Hamiltonian Monte Carlo approaches encounter a “minus-sign problem” that quickly degrades the accuracy of the results as the system size is increased. Several different approaches to overcome the minus-sign problem can be implemented, but none is robust across differing fermionic systems. There is clearly a great need for an improved numerical method for the study of large dynamical fermion problems in many fields of science.

Technical Approach

The DMRG is a promising alternative to conventional numerical methods in the study of large dynamical fermion problems.[1] This method scales favorably with system size when compared to exact diagonalization and has already been applied quite successfully to one-dimensional systems in condensed matter.[2] More recently the DMRG was also applied to problems in quantum chemistry and nuclear physics. The DMRG is based on a powerful truncation scheme that never lets the size of the problem get out of hand. Within DMRG, the model space is grown to very large sizes by the sequentially adding of more and more single-particle orbitals/lattice sites to the problem. Only the most important many-body states are kept, while less important states/correlations are truncated. The implementation of this algorithm is rather straightforward for spin chains and similarly homogeneous systems. For interacting many-body systems like quantum dots, questions concerning the optimal order of orbitals and partitioning of the model space arise. These issues influence the convergence of the method.

In our work we mainly followed the literature for DMRG application on spin chains.[1,2] However, we found that the convergence of the method improves notably when dimers (i.e., two spin-1/2 lattice sites) instead of individual lattice sites are used as elementary blocks. This procedure reduces the need of sweeps with the finite algorithm in the case of the spin-0 ground state of the alternating spin-1/2 antiferromagnetic Heisenberg chain. For the case of quantum dots, we restricted ourselves to two-dimensional spherical dots with harmonic confinement and transferred the ideas of Refs. 3 and 4 to our situation. In particular, we keep angular momentum as a good quantum number and use the Wilson renormalization group approach for the initial warm-up sweep. Orbitals are included corresponding to their distance from the Fermi surface. Particular care has to be taken to correctly implement the

Pauli principle. We developed both serial and MPI-based parallel codes for the DMRG algorithm. Standard library routines (BLAS, LAPACK, ARPACK) were used whenever possible to achieve both performance and portability.

Results and Accomplishments

We have developed a Fortran 90 program that solves a variety of interacting fermion problems using the DMRG algorithm. The main code was designed for single-processor machines, and a parallelized version has been tested and used on the high-performance computers of the Center for Computational Sciences (CCS) at ORNL. The program is portable and has been tested and used on a variety of computers (Compaq, IBM, Intel).

Spin Chains

We used our DMRG programs to study the critical behavior of the alternating spin-1/2 antiferromagnetic Heisenberg chain. This problem is of scientific interest since theoretical predictions for the critical exponents involve uncontrolled but widely accepted approximations that have to be checked numerically; it is also a numerical challenge due to the divergence of the correlation length and the necessary control of finite size effects. Considering increasingly long chains and decreasingly small alternation, we computed the critical exponents for the ground-state energy defect and the gap (see Fig. 1). Our numerical results are consistent with a pure power-law behavior. They agree with the theoretical predictions of power-law plus logarithmic corrections once we allow for a rather large (of order 100) and non-universal scaling parameter inside the logarithms.[5] We believe that our study is the most accurate numerical work on this subject. Our results may motivate further theoretical study to confirm the numerical values of our scaling parameters.

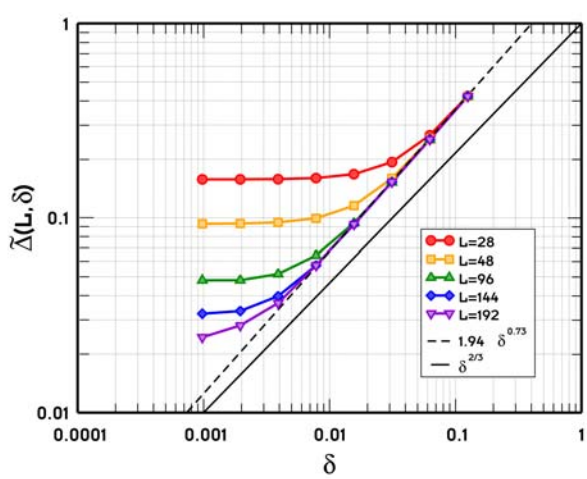

Fig. 1. Critical behavior of the singlet-triplet gap as a function of alternation d for spin chains of length L. *The dashed line shows a power law fit, which gives an exponent* $\delta = 0.73$. *The full line shows the renormalization-group exponent* $\delta = 2/3$.

Quantum Dots

We also performed numerical computations for two-dimensional spherical quantum dots with harmonic confinement and Coulomb interactions between the electrons. The DMRG algorithm converges toward the results of exact diagonalizations as the number of retained states is increased. This proof-of-principle shows that the DMRG is applicable also to interacting fermion problems in more than one dimension. However, the numerical effort is considerably larger for these systems than for the spin chains since the two-body interaction also couples distant single-particle orbitals and considerably more states have to be kept to obtain converged results. Further research is necessary to optimize the order of the single-particle orbitals and the algorithm for the initial sweep.

Nuclear Shell Model

We also applied the DMRG to nuclear shell model calculations. In these applications, the method encountered convergence problems due to difficulties during the warm-up phase of the algorithm. We hope to overcome these difficulties eventually. An analysis of this problem led two of us to propose and investigate a related method, the wave function factorization, for large-scale nuclear structure problems.[6]

Summary and Conclusions

Within this Seed Money Fund project, we developed a DMRG-based Fortran 90 program for numerical calculations in interacting fermion systems and applied it to computations in spin chains and quantum dots. The program is available for serial and parallel computers and is easily portable. We used the DMRG to study in detail the critical behavior of the alternating spin-1/2 antiferromagnetic Heisenberg chain. Our numerical results for the critical exponents of the gap and the ground-state energy defect agree with theoretical predictions provided rather large scaling parameters are introduced in the logarithms. They are the most accurate numerical results available for the study of this problem. We gave a proof-of-principle application of the DMRG to interacting electrons in harmonically confined spherical quantum dots. The results of this project open the avenue for a computational solution of different interacting fermion systems ranging from spin chains to quantum dots to atoms and molecules.

This project made the DMRG algorithm available within ORNL and thereby added to the Laboratory's competency in computational modeling of interacting

quantum systems. We presented the results of this project in seminars to the computational materials science group at ORNL's CCS and to the neutron scattering group at ORNL's High Flux Isotope Reactor (HFIR). Our DMRG program has already become useful inside ORNL: very recently, it was employed to interpret the data of a neutron scattering experiment at HFIR.[7]

References

[1]S. R. White, *Phys. Rev. Lett.* **69**, 2863 (1992).

[2]I. Peschel, X. Wang, M. Kaulke, and K. Hallberg (Eds.), *Density-Matrix Renormalization Group*, Springer, Berlin, 1999.

[3]G. Fano, F. Ortolani, and L. Ziosi, *J. Chem. Phys.* **108**, 9246 (1998).

[4]T. Xiang. *Phys. Rev. B* **53**, 10445 (1996).

[5]T. Papenbrock, T. Barnes, D. J. Dean, M. V. Stoitsov, and M. R. Strayer, *Phys. Rev. B* **68**, 024416 (2003).

[6]T. Papenbrock and D. J. Dean, *Phys. Rev. C* **67**, 051303(R) (2003).

[7]A. Zheludev, T. Masuda, B. Sales, D. Mandrus, T. Papenbrock, T. Barnes, and S. Park, eprint cond-mat/0310741.

Engineered Entanglement in Two-Photon States

V. A. Protopopescu, W. P. Grice, and Y.-H. Kim
Computer Science and Mathematics Division

The process of spontaneous parametric down-conversion (SPDC) is a convenient source of entangled photon pairs for use in various quantum information applications. For many of these applications, a pulsed source is required, but the polarization entanglement tends to suffer when the process is pumped by an ultrafast laser. Indeed, the experiments described below show that ultrafast-pumped SPDC produces pairs in which the photons have different spectral characteristics. We developed two methods for correcting the deleterious effects of these spectral differences. In the first, we specify the experimental parameters needed to produce a spectrally symmetric state, and in the second, we change the relationship between polarization and the distinguishing spectral information. Using the latter method, we have demonstrated the highest degree of polarization entanglement ever achieved in ultrafast-pumped type-II SPDC.

Introduction

The notion of entanglement was first introduced by Einstein, Podolsky, and Rosen (EPR) in a paper that analyzes the predicted measurement results in a *gedanken* experiment for a pair of specially correlated particles.[1] The quantum state of the pair is such that neither particle could be considered to be in a state independent of the other, regardless of the spatial separation of the two entities. Entangled states of two particles (photons) are most commonly generated in the process of type-II spontaneous parametric down-conversion (SPDC), in which a high-energy UV pump photon is split inside a nonlinear optical crystal into two orthogonally polarized lower-energy daughter photons. To date, most of the SPDC experiments have employed monochromatic (cw) lasers to pump the nonlinear crystals. With this type of pumping scheme, the emission time of a photon is highly correlated with that of its sibling since the photons are always emitted in pairs. The time at which a pair may be emitted, however, is completely random within the relatively long coherence time of the cw pump laser.

However, for applications such as the generation of multiphoton entangled states or quantum teleportation, well-timed photon pairs (within 100 fs) are a fundamental requirement. For other technologies, such as quantum cryptography, better timing control would represent an improvement over the state of the art. A seemingly natural solution is to use an ultrafast laser (femtosecond pulsed laser) to pump the SPDC process. Unfortunately, this method is not without its problems. The most notable of these is that the polarization entanglement in pulsed type-II SPDC is of poor quality; that is, the two-photon polarization state from SPDC pumped by an ultrafast laser behaves more like a mixed state, as opposed to a pure entangled state.[2]

From the study of the temporal and spectral properties of the two-photon wavefunctions, we found that the poorer quality of the polarization entanglement in pulse pumped type-II SPDC is likely due to differences between the group velocities of the photons involved in the SPDC process.[3] As a result, the two photons are emitted with different temporal and spectral properties. The primary objective of the project described herein was to develop a method for correcting the spectral dissimilarities and subsequently to provide the first experimental generation of high-intensity pulsed two-photon states maximally entangled in polarization. This was to be accomplished via a novel approach to the problem. Rather than passing the photons through narrow-band spectral filters in order to eliminate spectral differences (which would have reduced the count rates to very low levels), we sought to address the problem at the source by "engineering" a two-photon source to emit photons with the desired properties. A secondary objective was to verify the predictions of the theoretical treatments of ultrafast-pumped SPDC through the first-ever measurements of the joint spectrum of the two-photon state.

Technical Approach

In simplest terms, a polarization-entangled state consists of two photons whose polarizations are correlated in every measurement basis, even though their individual polarizations are undefined. The most direct method for the generation of such a state involves the geometric superposition of two definite polarization states emitted from a type-II SPDC crystal, yielding the state

$$|\psi\rangle = \frac{1}{\sqrt{2}}\left[|H\rangle_1|V\rangle_2 - |V\rangle_1|H\rangle_2\right],$$

where the subscripts denote two distinct directions of propagation and where H and V refer to horizontal and vertical polarization, respectively. In each path, a given photon may have either polarization, with the orthogonal polarization to be found in the conjugate path. A two-photon state constructed in this way may be considered maximally entangled only if the horizontally and vertically polarized photons are identical in all respects except polarization. If the polarization information is masked, it must be impossible to distinguish the two constituent terms.

As stated above, it is quite straightforward to generate maximally entangled photon pairs using cw-pumped SPDC. However, all efforts involving this type of technique have come up short when an ultrafast pump has been employed. Experimental studies have shown that such a method yields partially entangled states, with the degree of entanglement dependent on pump bandwidth and crystal length.[2] It had been suspected, but not directly confirmed, that the diminished entanglement was due to spectral and temporal differences between the two photons.[3,4] More precisely, the vertically polarized photons were suspected to have different properties from the horizontally polarized photons. An important task in this project was to experimentally verify these differences through the measurement of the joint spectrum. This measurement is relatively straightforward (albeit tedious), entailing simultaneous measurements of the spectra of the individual photons. The two photons were directed to two independent monochrometers monitored by single-photon detectors. The joint spectral intensity was then recorded as the normalized coincidence rate measured as a function of the wavelength settings of the two monochrometers. The data shown in Fig. 1 represent the first-ever measurements of the joint spectra of two-photon states. Measurements were made both for cw-pumped down-conversion [Fig. 1(a)] and for ultrafast pumped down-conversion [Fig. 1(b)]. The asymmetry in the second plot is a clear indication that the two photons have different spectral characteristics, even though their center wavelengths are identical.

The spectral asymmetry shown in Fig. 1(a) is the source of the poor polarization entanglement in ultrafast-pumped type-II SPDC. The theoretical treatments that predict this spectral structure also hold the key for overcoming the problem.[5] The asymmetry occurs because of the birefringence of the down-conversion crystal. The properties of the crystal determine the phase-matching conditions for the down-conversion process, that is, all of the ways that the energy of a pump photon may be distributed to the two daughter fields. Because the crystal is birefringent, the fields for the orthogonally polarized

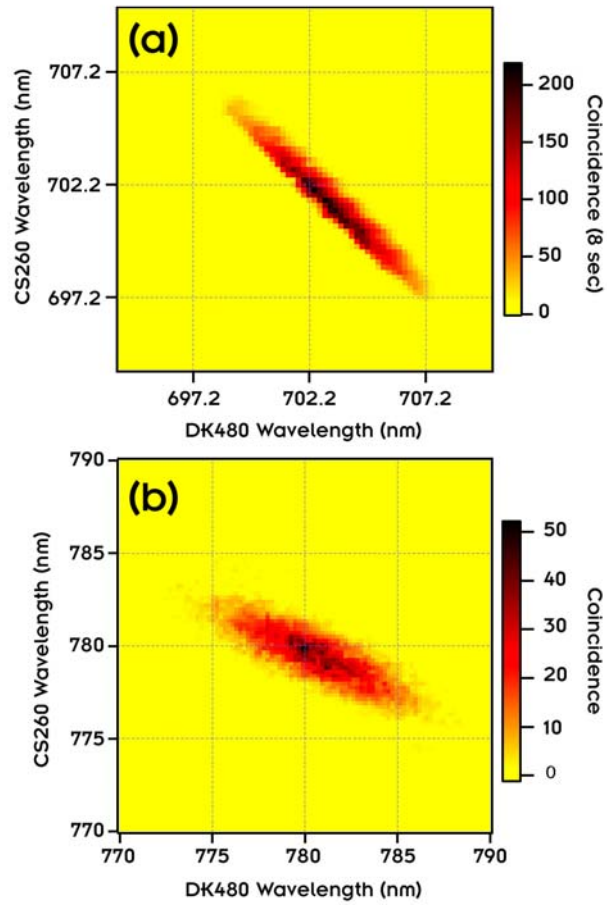

Fig. 1. Measured joint spectra for the two-photon states from (a) cw-pumped SPDC and (b) ultrafast-pumped SPDC.

photons are shaped by two different sets of crystal properties, resulting in an asymmetric phase-matching condition. This asymmetry is not seen in cw-pumped down-conversion because the very narrow pump field tends to "enforce" symmetry on the interaction. It is only when the pump bandwidth becomes large—as in ultrafast-pumped SPDC—that the asymmetry becomes apparent. Our approach to the problem was to examine the parameters affecting the down-conversion process in order to identify a configuration that would yield a symmetric phase-matching condition. It was found that the desired symmetry could be achieved if the group velocities of the three interacting fields satisfied the relation $v_{pump}^{-1} = \frac{1}{2}\left(v_1^{-1} + v_2^{-1}\right)$. After modeling several different crystal materials, a suitable candidate was found in beta barium borate (BBO) pumped at 757 nm. The calculated joint spectrum for this configuration, which is shown in Fig. 2, exhibits the desired symmetry.

An alternative approach for eliminating the effect of distinguishing spectral information was also developed during the course of this project. Here the idea is to permit

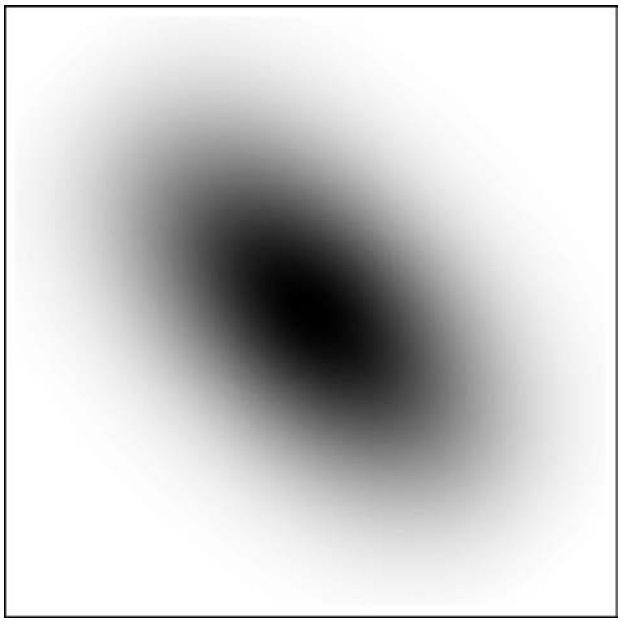

Fig. 2. Calculated joint spectrum with engineered symmetry.

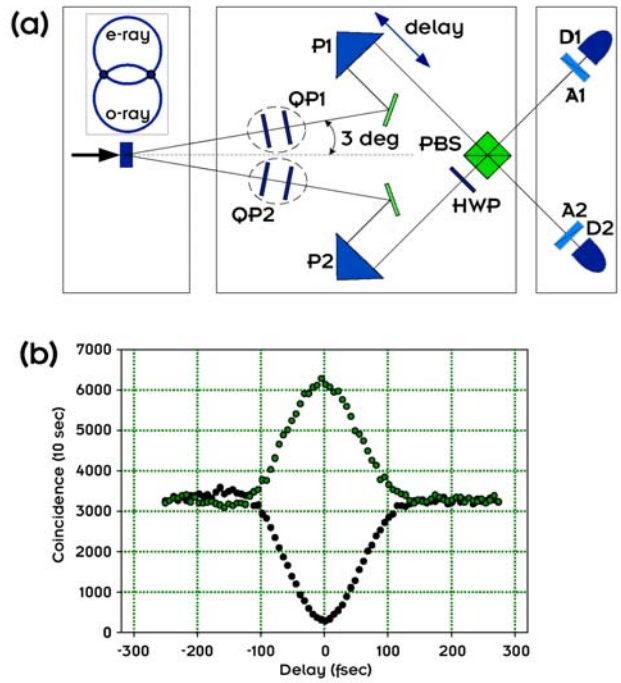

Fig. 3. (a) Two photons produced via ultrafast-pumped type-II SPDC meet at a polarization beamsplitter (PBS) after a half-wave plate (HWP) rotates the polarization in one arm by 90°. (b) Coincidence rates measured between detectors D1 and D2 as a function of delay. Polarization analyzers A1 and A2 were both set to 45° for the upper curve, while A2 was rotated to –45° for the lower curve.

spectral and temporal differences between the photons and focus, instead, on their correlation with polarization. By shifting the spectral correlation to path, rather than polarization, the spectral differences would yield no information regarding the polarization of a particular photon.[6] This "reassignment" of the correlation was accomplished in the set-up shown in Fig. 3(a). The photons exit the crystal as described above with a horizontally polarized photon in path 1 and a vertically polarized photon in path 2 ($|H\rangle|V\rangle$), or vice versa ($|V\rangle|H\rangle$). Before the photons are directed to a polarization beamsplitter (PBS), one of the photons has its polarization rotated by 90° so that the photons are identically polarized. Thus, they are either both reflected or both transmitted at the PBS, yielding the polarization-entangled state

$$|\psi\rangle_{\mathrm{OUT}} = \frac{1}{\sqrt{2}}\left[|H\rangle_1|H\rangle_2 - |V\rangle_1|V\rangle_2\right].$$

The important thing to note here is that the photon that exited the crystal with horizontal (vertical) polarization always ends up in path 1 (2). Only one set of spectral properties is present in each path, then, even though either polarization may be found. Thus, the spectral properties are correlated with path, rather than with polarization. This results in a high degree of polarization entanglement, as shown in Fig. 3(b). The two curves represent the coincidence rates as the photons are passed through crossed (lower curve) and parallel (upper curve) polarizers oriented at 45° with respect to the horizontal. When the path lengths are balanced (central region), the visibility is greater than 90%, indicating a high degree of polarization entanglement.

Results and Accomplishments

The work described above represents a number of important contributions to the fields of quantum optics and quantum information science. These are described in detail in six published papers[6,7] and two additional manuscripts either in preparation or under review.

The measurements of the joint spectra are notable for a number of reasons, not the least of which is that they are the first of their kind. As researchers progress from proof-of-principle experiments to real quantum applications (e.g., quantum cryptography, quantum computing, etc.), they will need to know more and more about the quantum states they use. For this reason, the joint spectrum measurement technique is expected to become an important tool. Extending the measurement to the temporal domain would enhance this capability even further, as it would enable the complete chrono-spectral characterization of the two-photon state. Another significant contribution to be attributed to the measurements of the joint spectra is the validation of the theoretical treatments of ultrafast-pumped SPDC. Prior to these measurements, the theory could be tested only indirectly. The data obtained and analyzed within this project provide a means to measure directly the spectral properties of the photon pairs and are in very good agreement with the theory.

Specification of the parameters needed for a symmetric joint spectrum is expected to be important for a number of quantum applications. Any application requiring a pulsed source of polarization-entangled photons will benefit, since a symmetric joint spectrum is needed for a high degree of polarization entanglement. In addition, it has recently been shown that photon pairs with a positively correlated joint spectrum can be used in quantum-enhanced clock synchronization. The positive correlation is possible only if the joint spectrum is symmetric.

Finally, the most significant contribution is likely to be the technique for redistributing distinguishing spectral information to transform mixed states into polarization-entangled states. Although this approach was not conceived before the project began, it is more subtle than the originally proposed method and still meets the stated objective of the project, namely, the first experimental generation of high-intensity pulsed two-photon states that are maximally entangled in polarization. Moreover, it meets this objective in a way that addresses the more general problem of managing information in entangled systems. Whatever form the first quantum computer takes, it is certain that the constituent systems will contain many degrees of freedom. In order to isolate the degree of freedom of interest, it will be necessary to control correlations with other variables in the system. In this case, the detrimental correlation between spectral properties and polarization (the degree of freedom of interest) was transformed to an innocuous correlation between spectral properties and path. We expect that this concept could be extended to other degrees of freedom and other systems. It is the generalization of this concept that is likely to have the most far-reaching effects.

A number of federal agencies are working toward the development of applications involving entangled photons. It is clear that the work described here will aid in those efforts, and several agencies have expressed interest. Quantum computing is being championed by the Defense Advanced Research Projects Agency. The National Reconnaissance Office has expressed interest in quantum-enhanced clock synchronization and in quantum cryptography. Also interested in quantum cryptography are the National Security Administration and the Advanced Research and Development Activity (ARDA). Based in large part upon the results obtained within this project, we have already obtained ARDA funding at the level of $150 K for the development of a pulsed two-photon source for quantum cryptography. Funding is expected to continue at this level for at least one more year.

Summary and Conclusions

Using a novel measurement technique developed for this project, it was shown that the spectral properties of the two photons produced in the process of ultrafast-pumped spontaneous parametric down-conversion are not identical, even when the center wavelengths are the same. These results provide the first direct validation of the multi-mode theory describing the process. Left unchecked, the spectral differences tend to reduce the degree of polarization entanglement achievable with the usual entangling techniques. Two methods have been developed to counteract these effects and improve polarization entanglement. In the first method, which is known as spectral engineering, the joint spectral properties of the photon pair are shaped through judicious choices of relevant experimental parameters. In the second method, the photons are allowed to retain their different spectral properties, but the spectral correlation with polarization is shifted to a correlation with direction of propagation. Using this technique, near-perfect polarization entanglement was achieved for the first time in ultrafast-pumped type-II down-conversion.

References

[1]A. Einstein, B. Podolsky, and N. Rosen, *Physical Review* **47**, 777 (1935).

[2]G. Di Giuseppe et al., *Phys. Rev. A* **56**, R21 (1997); W. P. Grice et al., *Phys. Rev. A* **57**, R2289 (1998).

[3]T. E. Keller and M. H. Rubin, *Phys. Rev. A* **56**, 1534 (1997).

[4]W. Grice and I. Walmsley, *Phys. Rev. A* **56**, 1627 (1997).

[5]Y.-H. Kim and W. P. Grice, *J. Mod. Opt.* **49**, 2309 (2002).

[6]Y.-H. Kim et al., *Phys. Rev. A* **67**, 010301(R) (2003).

[7]Y.-H. Kim and W. P. Grice, to appear in *Phys. Rev. A*; Y.-H. Kim, *Phys. Lett. A* **315**, 352 (2003); Y. H. Kim, *JOSA B* **20**, 1959 (2003); Y. H. Kim, *Phys. Rev. A* **68**, 013804 (2003); Y. H. Kim and W. P. Grice, *Phys. Rev. A* **67**, 065802 (2003).

Development of Readout Electronics Architecture for a Silicon-Strip Vertex Detector Upgrade to the PHENIX Experiment

V. Cianciolo, T. C. Awes, M. Bobrek, C. L. Britton, W. L. Bryan, K. F. Read, P. W. Stankus, A. L. Wintenberg, and G. R. Young
[1]*Physics Division*
[2]*Engineering Science and Technology Division*

The Relativistic Heavy Ion Collider (RHIC) at Brookhaven National Lab (BNL) smashes particle beams into each other in an attempt to create conditions of energy and density that have not existed since shortly after the Big Bang, thereby melting protons into their constituent quarks and gluons. The PHENIX experiment, one of the RHIC detectors which collects data on these collisions, has provided an intriguing series of results that has electrified the nuclear physics community. A multi-layer Silicon Vertex Detector would greatly extend PHENIX's scientific impact, and the goal of this project is to develop a viable concept for the outer layers of such a detector that meets stringent requirements on the detector thickness, radiation tolerance, and interfaces with a novel BNL-developed sensor and the PHENIX data acquisition system (DAQ).

A Silicon Vertex Detector would greatly extend the PHENIX scientific impact in the areas (key to characterization of the extreme conditions created in RHIC collisions) of suppression of particle production at large transverse momentum, suppression of quarkonia production, characterization of open heavy-flavor production, and gamma-tagged jet production.

Radiation damage concerns argue against using a double-sided silicon detector technology. Material thickness limits argue against multiple layers of silicon microstrip detectors in different orientations, and channel count argues against silicon pixel detectors. A novel alternative, developed by colleagues at BNL and RIKEN, is a strip-pixel detector which is essentially a pixel detector which has individual pixels ganged together into multiple strips on different metallization layers. This allows for two-dimensional readout with a single-sided process. Our goal was to develop a credible concept for the readout electronics that connected these sensors to the existing PHENIX DAQ.

Two options were available for the signal processing chip. The first was to a scheme based on a modification of the TGV family of application-specific integrated circuits (ASICs) developed previously by ESTD members of this project in conformance with PHENIX DAQ specifications and currently in use throughout PHENIX. An alternative was to use an ASIC (SVX4), developed by Fermi National Lab (FNAL), which might be suitable in its current form, thus eliminating the cost and risk associated with any chip development.

Through literature studies and extensive discussions with BNL and FNAL engineers we believe that the SVX4 will be compatible with both the sensor and with the PHENIX DAQ. We have also developed a small testboard that we will use to verify compatibility with the PHENIX DAQ. As a follow-on to this project, funds may be available from our Japanese colleagues to incorporate this testboard in a full system test (with a source and in a beam) of the sensor. We have evaluated the bandwidth requirements for the system and found design options compatible with the existing data-collection modules (DCMs) and with proposed DCM upgrades. We have evaluated the minimum thickness that a detector based on these sensors is likely to require. The result is that more material is required than desired—this information is being incorporated into simulations of the entire PHENIX detector and preliminary indications are that the required amount of material is acceptably small. Similarly we have determined that the SVX4 alternative does not have event selection (triggering) capability before digitization. Again, this information is being incorporated into simulations of the entire PHENIX detector and preliminary indications are that such triggering is not necessary. Finally, we have developed a novel concept for the bus required to bring signals and power to and from the signal processing chips. This concept greatly simplifies assembly and reduces the amount of material in the detector of the detector and readout electronics.

Toward Neutron Star Merger Simulations: Gravitational Waves, Heavy Element Nucleosynthesis, and Gamma-Ray Bursts

C. Y. Cardall,[1,2] M. W. Guidry,[1,2] A. Mezzacappa,[1] and R. J. Toedte[3]
[1]*Physics Division*
[2]*The University of Tennessee*
[3]*Computer Science and Mathematics Division*

Neutron star mergers are associated with three phenomena of high interest in astrophysics: gravitational waves, heavy element nucleosynthesis, and gamma-ray bursts. Advanced simulation and analysis tools are needed to shed light on neutron star mergers and their phenomenology. Our objective in this project is to develop a set of computational tools, *GenASiS* (*Gen*eral *A*strophysical *Si*mulation *S*ystem), that will position us to study neutron star mergers with massively parallel simulations on distributed memory computer architectures. As initial stages to *GenASiS*, we are developing an adaptive-mesh radiation hydrodynamics code with self-gravitation and associated visualization tools.

The purpose of this project is to seed the development of a program to study neutron star mergers with massively parallel simulations on distributed memory computer architectures.

Neutron star mergers feature two self-gravitating bodies composed of dense nuclear matter, moving at high speed; this calls for adaptive-mesh radiation hydrodynamics, a frontier in scientific computing. The idea of an adaptive mesh is to employ high resolution only where needed in order to conserve memory and computational effort. In this problem, an adaptive mesh would allow much of the "empty space" between the two neutron stars to be handled with low resolution. Radiation transport is so expensive—both in terms of memory and computational demands—that an adaptive mesh is the only way it could be implemented in three spatial dimensions. Adaptive-mesh refinement for hydrodynamics had been around for some time, but adaptive-mesh refinement for radiation hydrodynamics remains a frontier to which significant contributions can be made.

Before this project began in June 2003 we had begun developing *GenASiS* (*Gen*eral *A*strophysical *Si*mulation *S*ystem), an adaptive-mesh neutrino radiation hydrodynamics code; our work in this project will bring *GenASiS* to a level of development that will permit credible proposals to simulate neutron star mergers. The project is to be completed in FY2004. We have four tasks:

1. Parallelize our adaptive-mesh hydrodynamics code and add a realistic dense nuclear matter equation of state. By the end of FY2003 we had added the realistic equation of state, written code that partitions the mesh in such a way that each processor has its share of spatial zones at each level of refinement, and written code that exchanged mesh refinement and coarsening information between all processors.
2. To include self-gravity, we must implement a Poisson solver on adaptive mesh. At the end of FY 2003 we had worked out the finite differencing of the Poisson equation on an adaptive mesh in coordinates sufficiently general to allow Cartesian, spherical, and cylindrical coordinates to be used. We have also become familiar with Portable, Extensible Toolkit for Scientific computation (PETSc), whose routines we will use to solve the distributed sparse matrix system resulting from the finite differenced Poisson equation.
3. Add realistic neutrino interactions to our parallel, fixed-mesh neutrino radiation transport code; incorporate number and energy transfer to the fluid; and make this code adaptive. Our work in FY 2003 focused on adding realistic interactions and number and energy transfer. The realistic interactions are being implemented using the GlobalArrays library to distribute segments of the high-dimensional interaction kernels among processors; code has been written which allows each processor to grab the pieces of the table it needs. Code infrastructure to handle number and energy transfer is partially completed.
4. Implement visualization tools for our adaptive mesh. This work will take place in FY2004.

In addition to enabling a program of neutron star merger studies, this work has many benefits to DOE and other agencies. It addresses DOE's need for research in advanced scientific computing. Moreover, neutron star mergers involve interesting nuclear physics issues, including the dense matter equation of state, neutrino

interactions, and heavy element (r-process) nucleosynthesis (the subject to be studied by the Rare Isotope Accelerator proposed to DOE). Developments in radiation transport are useful in studies of combustion, climate, and stockpile stewardship—all of interest to DOE. This project also will be relevant to projects undertaken by the National Science Foundation (NSF) and the National Aeronautics and Space Administration (NASA). The NSF is funding the Laser Interferometer Gravitational Wave Observatory that is comprised of two detectors of gravitational radiation from astrophysical sources. Neutron star mergers are expected to be a primary source of gravitational waves, and "templates" computed from simulations that are needed to distinguish gravitational wave signals from noise. The NSF is also funding a Physics Frontier Center for gravitational wave phenomenology at Penn State, to which our work will also contribute. NASA has several orbiting observatories, both active and planned, sensitive to various wavelengths of electromagnetic radiation; these study the enigmatic gamma-ray bursts, of which neutron star mergers are one of two proposed "central engines."